Optimal Estimation of EMG Standard Deviation (EMGσ) in Additive Measurement Noise: Model-Based Derivations and Their Implications

Haopeng Wang, Kiriaki J. Rajotte, He Wang, Chenyun Dai, Ziling Zhu, Moinuddin Bhuiyan, Xinming Huang, *Senior Member, IEEE*, and Edward A. Clancy, *Senior Member, IEEE*

***Abstract*— Typical electromyogram (EMG) processors estimate EMG signal standard deviation (EMGσ) via moving average root mean square (RMS) or mean absolute value (MAV) filters, whose outputs are used in force estimation, prosthesis/orthosis control, etc. In the inevitable presence of additive measurement noise, some processors subtract the noise standard deviation from EMG RMS (or MAV). Others compute a root difference of squares (RDS)—subtract the noise variance from the square of EMG RMS (or MAV), all followed by taking the square root. Herein, we model EMG as an amplitude-modulated random process in additive measurement noise. Assuming a Gaussian (or, separately, Laplacian) distribution, we derive analytically that the maximum likelihood estimate of EMGσ requires RDS processing. Whenever that subtraction would provide a negative-valued result, we show that EMGσ should be set to zero. Our theoretical models further show that during rest, approximately 50% of EMGσ estimates are non-zero. This result is problematic when EMGσ is used for real-time control, explaining the common use of additional thresholding. We tested our model results experimentally using biceps and triceps EMG from 64 subjects. Experimental results closely followed the Gaussian model. We conclude that EMG processors should use RDS processing and not noise standard deviation subtraction.**

***Index Terms*— Biological system modeling, biomedical signal processing, electromyogram, electromyogram (EMG) amplitude estimation, electromyography, myoelectric signal processing.**

I. Introduction

THE surface electromyogram (EMG) interference pattern has commonly been processed by the cascade operations of highpass filtering (to remove DC offsets and attenuate motion artifacts); optional pre-whitening [1]–[3]; and then taking its moving average root mean square (RMS), moving average mean absolute value (MAV), or by rectifying the signal followed by lowpass filtering. If EMG is modeled as an amplitude-modulated random process, then these schemes estimate its time-varying standard deviation (EMGσ). For constant-force, non-fatiguing contractions, it has been shown that RMS processing is the optimal estimate of EMGσ if the *noise-free* EMG signal is modeled as Gaussian distributed [2], [4]–[6], and that MAV processing is optimal if the *noise-free* EMG signal is modeled as Laplacian distributed [7]. EMGσ has been used to estimate torque [8]–[13] and mechanical impedance about a joint [14]–[19], in motor control research [20], and in applications including prosthesis control [21]–[23], ergonomics [24], [25] and biomechanics [26], [27].

However, EMG is always measured in the presence of additive measurement noise, i.e., noise that exists independent of the level of muscle effort. This noise arises from the measurement apparatus (thermal and active device noise), radiated electromagnetic interference, electrode-to-skin contact resistance [28], unrelated electrophysiological activity, etc. [29]. This noise has an average RMS intensity that is 1.1–4.5% of the RMS EMG at maximum voluntary contraction (MVC) [3], [8], [9], [30]–[34]. Consequently, the signal to noise ratio (SNR) is low at low contraction levels.

Thus, researchers have proposed alterations to their EMG processors and/or models to include noise. Kaiser and Peterson [1] found that the shape of their whitening filter should be a function of the contraction level, with lower high-frequency gain during low contraction levels. Parker *et al.* [35], Zhang *et al.* [36], and Parker and Scott [37] modeled noise as an additive (white Gaussian) process when *solving* for an optimal multistate EMG classifier, and when *analyzing* (but not *solving*) EMGσ estimators. This additive noise model is now common (e.g., [3], [38]–[40]). Clancy and Farry [3] whitened the raw EMG, then attenuated additive noise using an adaptive Wiener filter. A Weiner filter is the optimal *linear* filter for attenuating additive noise, but is not necessarily the optimal filter overall. Many papers within the ergonomics literature routinely subtract the standard deviation of the background noise from RMS (or MAV) estimates [41]. However, it has

Manuscript received August 18, 2019; revised October 10, 2019; accepted October 24, 2019. Date of publication November 4, 2019; date of current version December 6, 2019. *(Corresponding author: Edward A. Clancy.)*

H. Wang, K. J. Rajotte, H. Wang, Z. Zhu, X. Huang, and E. A. Clancy are with the Department of Electrical and Computer Engineering, Worcester Polytechnic Institute, Worcester, MA 01609 USA (e-mail: hwang10@wpi.edu; kjrajotte@wpi.edu; hwang9@wpi.edu; zzhu2@wpi.edu; xhuang@wpi.edu; ted@wpi.edu).

C. Dai is with the Department of Electrical Engineering, Fudan University, Shanghai 200433, China (e-mail: chenyundai@fudan.edu.cn).

M. Bhuiyan is with the Department of Electrical and Computer Engineering and Computer Science, University of New Haven, West Haven, CT 06516 USA (e-mail: mbhuiyan@newhaven.edu).

Digital Object Identifier 10.1109/TNSRE.2019.2951081

been theoretically *argued* [42], [43] that the root difference of squares (RDS) [i.e., subtracting the noise variance from the square of EMG RMS (or MAV), all followed by taking the square root] is the correct approach. An experimental comparison found that RDS processing performs better than standard deviation subtraction [44].

The argument for RDS processing is based on the fact that if the signal and noise are independent, then their variances add—*in theory*. However, to our knowledge, this proposed processor has not been *derived* (i.e., *solved* for, based on a model) as a statistical estimator in the published literature (although one unpublished preliminary result appears in [45]). Solution via an estimator can demonstrate the optimality (or lack thereof) of a processor and expose its statistical properties. Herein, we provide this derivation, some of its properties and experimental evaluation of the derived optimal results, all for the case of constant-effort contraction.

II. Mathematical Models of EMG in Additive Noise

Consider an amplitude modulated model of the measured EMG signal, $m[n]$, during constant-effort contraction as [2], [5], [35]–[37]:

$$m[n] = s \cdot x[n] + v[n], \quad 0 \le n < N \tag{1}$$

where n is the discrete-time sample index, $s \equiv EMG\sigma$ is the standard deviation (i.e., modulation) of the noise-free EMG, $(s \cdot x[n])$ is the noise-free EMG signal and $v[n]$ is additive noise. Let $x[n]$ be zero mean, unit-variance, wide-sense stationary, correlation-ergodic and have independent samples (i.e., via pre-whitening). Let $v[n]$ be similarly specified, but of variance equal to q^2 and independent of $x[n]$. Let $\underline{m}$, $\underline{x}$ and $\underline{v}$ be vectors comprised of N successive samples of each respective random variable.

A. Gaussian Model—EMGσ Estimate [45], [46]

Let both $\underline{x}$ and $\underline{v}$ be jointly Gaussian. Then, $\underline{m}$ is jointly Gaussian with zero mean and covariance matrix: $K_{\underline{mm}} = \sigma_m^2 I$, where $\sigma_m^2 = s^2 + q^2$ and I is the identity matrix. Thus, the probability density function (PDF) for $\underline{m}$, given that the standard deviation of the noise-free EMG is $s \equiv EMG\sigma$, is:

$$p_{\underline{m}|s}\left(\underline{M}|s\right) = \frac{e^{\frac{-\underline{M}^T K_{\underline{mm}}^{-1} \underline{M}}{2}}}{(2\pi)^{N/2}\left|K_{\underline{mm}}\right|^{1/2}} = \frac{e^{\frac{-\sum_{n=0}^{N-1} M^2[n]}{2\left(s^2+q^2\right)}}}{\left[2\pi\left(s^2+q^2\right)\right]^{N/2}}, \tag{2}$$

where $\underline{M}$ denotes an instance of the random vector $\underline{m}$.

The maximum likelihood (ML) estimate of s is the value $\hat{s}$ which maximizes the above PDF. A monotonic transformation of the PDF does not alter the location of the maximum. Thus, taking the natural logarithm yields:

$$\ln\left[p_{\underline{m}|s}\left(\underline{M}|\hat{s}\right)\right] = -\frac{N}{2}\ln(2\pi) - \frac{N}{2}\ln\left(\hat{s}^2+q^2\right) - \frac{\sum_{n=0}^{N-1} M^2[n]}{2\left(\hat{s}^2+q^2\right)}. \tag{3}$$

Differentiating the above with respect to $\hat{s}$ gives:

$$\frac{\partial \ln\left[p_{\underline{m}|s}\left(\underline{M}|\hat{s}\right)\right]}{\partial \hat{s}} = -\frac{N}{2}\frac{2\hat{s}}{\hat{s}^2+q^2} + \frac{\hat{s}\sum_{n=0}^{N-1} M^2[n]}{\left(\hat{s}^2+q^2\right)^2}. \tag{4}$$

Setting this derivative to zero and manipulating leads to a quadratic equation for $\hat{s}^2$, the square root of which provides our intermediate result. The quadratic equation has two solutions. But, one of these solutions is not real-valued, so can be eliminated. The retained intermediate result, written as a discrete-time filter, is:

$$\hat{s}[n] = \sqrt{\left(\frac{\sum_{i=0}^{N-1} M^2[n-i]}{N}\right) - q^2}. \tag{5}$$

The parenthesized term within the square root is the mean square value. Hence, the noise correction is made via RDS processing.

The second derivative of (3) with respect to $\hat{s}$, evaluated at the location of the intermediate result specified by (5) is:

$$\frac{\partial^2 \ln\left[p_{\underline{m}|s}\left(\underline{M}|\hat{s}\right)\right]}{\partial \hat{s}^2} = \left[\frac{2N^3}{\left(\sum_{i=0}^{N-1} M^2[n-i]\right)^2}\right] \cdot \left[q^2 - \frac{\sum_{i=0}^{N-1} M^2[n-i]}{N}\right]. \tag{6}$$

This second derivative is less than or equal to zero, indicating a local maximum (and *not* a minimum), when $\frac{1}{N}\sum_{n=0}^{N-1} M^2[n-i]$ exceeds the noise variance q^2. This condition is almost always satisfied during active muscle contraction, but not during low-level contractions or rest. When the condition is not satisfied, maximization with respect to $\hat{s}$ of the PDF occurs at the boundary constraint where $\hat{s} = 0$ [47]. Hence, the complete solution for this ML estimate is:

$$\hat{s}_{\mathrm{RMS}}[n] = \sqrt{\max\left[0, \left(\frac{\sum_{i=0}^{N-1} M^2[n-i]}{N}\right) - g^2 q^2\right]}, \tag{7}$$

where "max" denotes the maximum value operator and the "RMS" subscript emphasizes the use of an RMS processor. Constant scaling factor g has been inserted into this solution, since some applications prefer to artificially inflate the noise threshold. For example, in myoelectric prosthesis control, $g > 1$ helps to insure that the prosthesis is not actuated during rest. For the optimum ML estimate, $g = 1$.

Denote the term in the rounded parenthesis of (7) (i.e., the mean square value of the measured EMG signal) as y. This random variable is Gamma distributed as:

$$p_y(Y) = \frac{Y^{\frac{N}{2}-1} e^{\frac{-Y \cdot N}{2\sigma_m^2}}}{\left(\sigma_m\sqrt{\frac{2}{N}}\right)^N \Gamma\left(\frac{N}{2}\right)}\mu(Y), \tag{8}$$

where $\Gamma(\cdot)$ is the Gamma function and $\mu(\cdot)$ is the step function. Its cumulative density function (CDF) is:

$$P_{y\le}(Y) = 1 - \sum_{k=0}^{\frac{N}{2}-1} \frac{\left(\frac{N}{2\sigma_m^2}\right)^k Y^k e^{\frac{-Y \cdot N}{2\sigma_m^2}}}{k!}\mu(Y), \quad N \text{ even}. \tag{9}$$

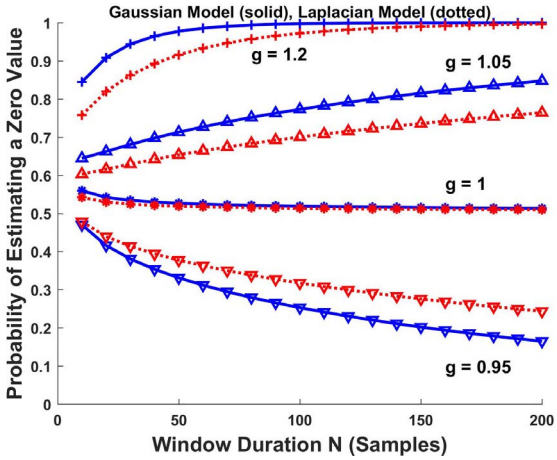

Fig. 1. Probability of estimating a zero EMGσ value during rest for theoretical Gaussian model (moving average RMS processing; solid blue) and Laplacian model (moving average MAV processing; dashed red) as a function of number of independent samples N, for four different noise gain values "g".

When the muscle is at rest, the true EMGσ is zero ($s = 0$) and the variance of the measured EMG signal is $\sigma_m^2 = q^2$. A fraction of the EMGσ estimates—but not all—will be zero (due to the noise variance subtraction). This probability of estimating a zero value during rest is the CDF of y, evaluated at $Y = g^2q^2$ (with $s = 0$). This probability, for N even, is:

$$P_{y\le g^2q^2,Rest}(Y) = \left[1 - \sum_{k=0}^{\frac{N}{2}-1} \frac{\left(\frac{N}{2}\right)^k g^{2k} e^{\frac{-g^2N}{2}}}{k!}\right] \mu(Y). \quad (10)$$

Note that this probability is *not* a function of the noise variance and is *only* a function of N and g. Fig. 1 shows this probability as a function of N for four possible values of g. Equation 10 and Fig. 1 show that for $g > 1$, a negative-valued subtraction result within (7) is more likely, producing a higher probability of estimating $\hat{s} = 0$. Conversely, for $g < 1$, a negative-valued subtraction result is less likely, producing a lower probability of estimating $\hat{s} = 0$.

B. Laplacian Model—EMGσ Estimate [7], [45], [46]

MAV processing has been shown to be the ML estimate of EMGσ, if the PDF is Laplacian [7]. So that the additive noise model has a Laplacian PDF, we directly model the measured EMG samples $m[n]$ as being independent and of a Laplacian PDF, without explicit specification of the PDFs of $x[n]$ and $v[n]$. (Note that if $x[n]$ and $v[n]$ are each modeled as Laplacian, then their sum is *not* Laplacian.) Nonetheless, if $x[n]$ and $v[n]$ are assumed independent, then their variances again add. Thus, the measured EMG again has variance: $s^2 + q^2$, and the PDF for sample $m[n]$ is [48]:

$$p_{m[n]|s}(M[n]|s) = \frac{\sqrt{2}}{2} \cdot \frac{e^{\frac{-\sqrt{2}}{(s^2+q^2)^{1/2}}|M[n]|}}{(s^2+q^2)^{1/2}}. \quad (11)$$

Since the samples of the EMG vector $\underline{m}$ are independent, its joint PDF is the product of the N individual PDFs, which simplifies to:

$$p_{\underline{m}|s}(\underline{M}|s) = \left[\frac{\sqrt{2}}{2(s^2+q^2)^{1/2}}\right]^N e^{\frac{-\sqrt{2}}{(s^2+q^2)^{1/2}}\sum_{n=0}^{N-1}|M[n]|}. \quad (12)$$

Similar to the Gaussian case above, maximum likelihood estimation of s is found by taking the natural logarithm of the PDF, differentiating with respect to $\hat{s}$, setting this derivative to zero and solving for $\hat{s}$. Again, the second derivative proves this intermediate result to, in fact, be a minimum, subject to the same boundary constraint where $\hat{s} = 0$. The complete filter for this ML estimate, again inserting a scaling factor g for the noise, is:

$$\hat{s}_{MAV}[n] = \sqrt{\max\left[0, \left\{\left(\frac{\sqrt{2}}{N}\sum_{i=0}^{N-1}|M[n-i]|\right)^2\right\} - g^2q^2\right]}. \quad (13)$$

Denote the term in the curly brackets of (13) as w. The PDF for this random variable is:

$$p_w(W) = \frac{e^{-\frac{N\sqrt{W}}{\sigma_m}}}{2} \cdot \left[\sum_{k=0}^{N-1}\left(\left\{\frac{N}{\sigma_m\sqrt{W}} - \frac{(N-1-k)}{W}\right\} \cdot \prod_{p=1}^{N-1-k}\left\{\frac{N\sqrt{W}}{\sigma_m p}\right\}\right)\right]\mu(W). \quad (14)$$

Its CDF is:

$$P_{w\le}(W) = \left\{1 - e^{-\frac{N\sqrt{w}}{\sigma_m}}\left[\sum_{k=0}^{N-1}\left(\prod_{p=1}^{N-1-k}\frac{N\sqrt{W}}{\sigma_m p}\right)\right]\right\}\mu(W). \quad (15)$$

The probability of estimating a zero value during rest is the CDF evaluated at $W = g^2q^2$ (with $s = 0$):

$$P_{w\le g^2q^2,Rest}(W) = \left\{1 - e^{-Ng}\left[\sum_{k=0}^{N-1}\left(\prod_{p=1}^{N-1-k}\frac{Ng}{p}\right)\right]\right\} \cdot \mu(W). \quad (16)$$

Again, the probability of a zero value is only related to N and g. Fig. 1 shows this probability as a function of N for four possible values of g.

III. Experimental Evaluation of the Models

A. Experimental Data Set

Data from 64 subjects acquired during four prior experiments with overlapping protocols were used for this study [3], [8], [30], [33]. Re-analysis of these data was exempted from human studies supervision by the WPI Institutional Review Board. Subjects had no known neuromuscular deficits of the right shoulder, arm or hand. In each experiment (see Fig. 1 in [8] for a photograph of the most recently used experimental apparatus), a subject was seated and secured with seat belts. Their right shoulder was abducted 90°, elbow flexed 90°, and hand supinated perpendicular to the floor. Their wrist was cuffed to a load cell to measure constant-posture elbow torque.

The skin above the triceps and biceps muscles was scrubbed with an alcohol wipe. Gel was applied in the latter two studies. Four bipolar EMG electrode-amplifiers were secured over each of the triceps and biceps muscles, in a tightly-spaced transverse row centered on the muscle mid-line, midway between the elbow and the midpoint of the upper arm. Each electrode-amplifier had stainless steel, hemispherical contacts of diameter 4 or 8 mm, separated 10 mm edge-to-edge, oriented along the long axis of the muscle. A reference electrode was secured alongside the active electrodes. Each EMG channel had selectable gain, a CMRR $\geq$ 90 dB at 60 Hz, a 10 or 15 Hz highpass filter (second or fourth order), and a 1800 or 2000 Hz lowpass filter (fourth order). EMG and load cell data were sampled at 4096 Hz at 16-bit resolution. Achieved force was fed back in a real-time display, along with a force target.

After a brief warm-up, separate elbow flexion and extension maximum voluntary contraction (MVC) forces were measured, without the use of force feedback. At least 20–30 minutes had elapsed between the time at which the electrodes were mounted and the completion of these MVC measurements. Then, constant-force 50% MVC extension trials, 50% MVC flexion trials and 0% MVC trials (arm at rest, removed from the wrist cuff) were acquired for 5 s each, using force feedback. (Only one of each type of trial was used in our analysis.) Two or three minutes of rest was provided between trials to avoid cumulative fatigue. Each of the eight, 5-s duration EMG signals from a trial was defined as an "epoch." Before any further use off-line, each epoch was highpass filtered (15 Hz cut-off, fourth-order Butterworth); IIR notch filtered at 60 Hz and its harmonics (second-order); when selected, adaptively pre-whitened [3], [49]; and bandlimited to 600 Hz [50] (fourth-order Butterworth lowpass). Then the first 500 ms of each epoch was omitted to account for filter start-up transients.

B. Evaluating Model Assumptions—EMG PDF

We evaluated the model assumptions related to the first-order PDF of EMG, both at rest and during 50% MVC trials, with and without whitening. During 50% extension trials, only the four epochs from triceps electrodes were examined; during 50% flexion trials, only the four epochs from biceps electrodes were examined. A total of 512 epochs (64 subjects $\times$ 8 electrodes/subject) were available at 0% (rest) and at 50% MVC (combining extension and flexion). Each EMG epoch was normalized to a sample variance of one and a histogram PDF estimate formed (500 bins, equally spaced over the range from -5 to $+5$). The ensemble histogram sample means and standard deviations are shown in Fig. 2.

Best matching between the ensemble vs. theoretic Gaussian/Laplacian PDFs did *not* occur when using theoretic PDFs of unit variances. Thus, the absolute error difference between each ensemble and theoretic PDF was computed for theoretic PDF standard deviations between 0.5 and 2 (increment of 0.01). The minimum area and its corresponding theoretic PDF standard deviation are shown in Table I (see also Fig. 2). In all cases, the data more closely followed the Gaussian model. Kolmogorov-Smirnoff tests between the experimental ensemble PDFs and each of the Gaussian and Laplacian PDFs were not sensitive, finding no statistically significant differences using either the Gaussian model ($p > 0.99$) or the Laplacian model ($p > 0.31$), for the four combinations of effort level (0% MVC, 50% MVC) and whitening. Thus, we computed the absolute area difference between each of the 512 histogram PDF estimates vs. the Gaussian/Laplacian PDFs, finding the best fit standard deviation for each. Paired sign tests (Bonferroni corrected) found the Gaussian PDF to be a better fit $\left(p < 10^{-6}\right)$ for each of the four combinations.

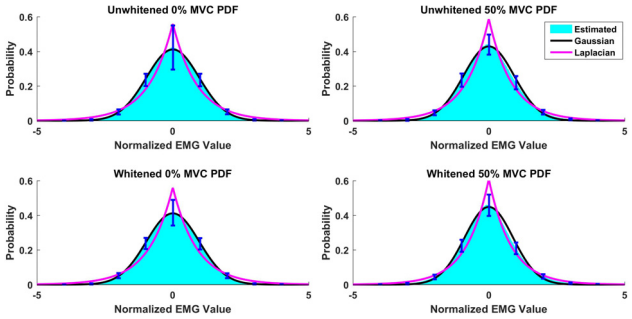

Fig. 2. Top shows ensemble-average PDF estimates of *unwhitened* EMG during 0% MVC (left) and 50% MVC (right), as well as best-fit theoretic Gaussian and Laplacian PDFs. Bottom shows corresponding PDF estimates from *whitened* EMG. $N = 512$ epochs from 64 subjects. Error bars in each plot show ± 1 std. dev. for the ensemble-average estimates.

TABLE I
ABSOLUTE AREA DIFFERENCES BETWEEN EXPERIMENTAL ENSEMBLE PDFS AND GAUSSIAN/LAPLACIAN PDFS. PARENTHESES LIST STANDARD DEVIATION AT WHICH AREA DIFFERENCE WAS ASSESSED (I.E., STANDARD DEVIATION AT WHICH THE ABSOLUTE ERROR DIFFERENCE BETWEEN EACH ENSEMBLE AND THEORETIC PDF WAS MINIMIZED)

EMG	Gaussian Model		Laplacian Model	
Processing	0% MVC	50% MVC	0% MVC	50% MVC
Unwhite	0.0241 (0.97)	0.0530 (0.93)	0.1981 (1.26)	0.1730 (1.20)
White	0.0188 (0.97)	0.0749 (0.89)	0.2035 (1.26)	0.1532 (1.16)

C. Evaluating Estimates of EMGσ

Historically, quantitative evaluation of constant-effort EMGσ has used the ratio of the estimate mean to its standard deviation (the inverse of the coefficient of variation), denoted the SNR. With this definition, variations about the mean of EMGσ are considered as "noise." This definition was convenient, as knowledge of neither the "true" EMGσ value nor the EMGσ-force relationship was necessary, and the measure is invariant to signal gain. However, that definition is not as indicative of EMGσ estimate performance once additive noise is modeled. In particular, the noise can cause the EMGσ estimate to incorrectly coalesce about the wrong mean value. In this case, SNR would measure the variation of the processed signal *plus* noise; and not the desired error with respect to the true (noise-free) EMGσ—which is more appropriate for this study.

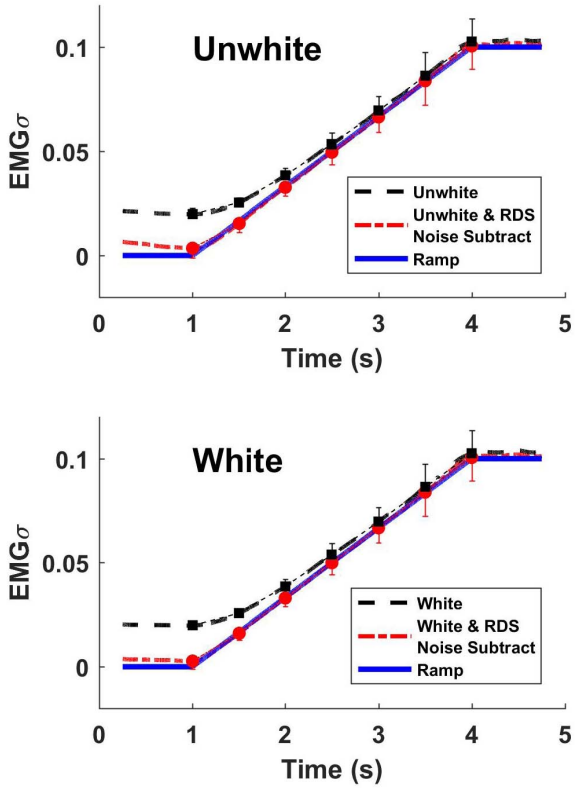

Fig. 3. Top shows ensemble averaged *unwhitened* EMGσ estimates along the ramp contraction, with and without RDS processing. Symbols and one-sided error bars show mean and one standard deviation at times 1.0, 1.5, 2.0, . . ., 4.0. Bottom shows corresponding results for *whitened* EMGσ estimates.

Thus, root mean square error between the true and estimated EMGσ value was used as the error measure. However, the true value is not known when assessing with real EMG data. Thus, we pursued an approach similar to [41]. Our available 50% MVC trials assume that muscle effort—and therefore EMGσ—is not changing during the contraction. So, we optionally whitened each EMG epoch, then normalized each 0% and, separately, each 50% MVC epoch to have a standard deviation of one. We treated each 50% MVC epoch as the "true" EMG signal and its 0% MVC epoch from the corresponding electrode as noise. We then multiplied each normalized 50% MVC EMG epoch point-by-point by a ramp (1 s zero, 3 s ramping from 0 to 0.1, 1 s at 0.1). To this signal, we added 0.02 times the respective, normalized 0% MVC epoch. This addition gave a SNR of 5, which is representative of measured EMG [3], [8], [9], [30]–[34]. We then computed the EMGσ estimate using a 200 ms duration centered (non-causal) window, only using RMS processing (since the Gaussian model was a much better fit to our data), with and without RDS processing. The root mean square error between the EMGσ estimate and the "true" EMGσ (i.e., the ramp pattern) was computed at times 1.0, 1.5, . . . 4.0 s across the 512 epochs (64 subjects $\times$ 8 electrodes per subject). Fig. 3 shows summary results. Due to non-normality of the data, we computed paired sign tests (separately for each time) between the root mean square error of all six unique paired combinations of the four factors: unwhitened data, whitened data, without RDS processing, and with RDS processing (Bonferroni corrected). Comparing each method with RDS processing to each method without RDS processing (four comparisons) always resulted in significantly lower errors *with* RDS processing for times $\leq$2.5 s $\left(p < 10^{-5}\right)$, and no differences for times $\geq$3 s $(p > 0.1)$. When unwhitened vs. whitened processors were compared *without* RDS processing (one combination), there were no statistical differences $(p > 0.1)$, except at 1.5 s $\left(p = 10^{-4}\right)$—likely an anomoly. When unwhitened vs. whitened processors were compared *with* RDS processing (one combination), whitening had lower error for times $\leq$1.5 s $\left(p < 10^{-5}\right)$, and was not significantly different for times $\geq$3.0 s $(p > 0.1)$.

D. Evaluating Probability of a Zero Value at Rest

The theoretical results predict that the probability of estimating a zero value for EMGσ during rest is a function of the window length and the noise gain factor "g". We experimentally evaluated this result using the 512 0% MVC epochs. We again limited analysis to RMS processing. We computed the fraction of zero-valued estimates when using RDS processing for all combinations of: unwhitened vs. whitened processing, window length values ranging from N = 2–400 ms, and g values of 0.95, 1, 1.05 and 1.2. The sample variance of each rest epoch was computed (after removing a 400 ms startup transient) and used as the noise variance q^2 to compute its respective RMS estimate of EMGσ.

With this method, the selected window length is misleading for comparison to the theoretical results shown in Fig. 1, because the experimental EMG signal is correlated (i.e., has finite bandwidth). To resolve this conflict, Hogan and Mann [4] and Bendat and Piersol [51] list the number of effective independent samples for a correlated Gaussian process as: $N_{Eff} = 2B_S T$, where B_S is statistical bandwidth (Hz) and T is the window duration (s). Thus, we used the method of [52] to estimate statistical bandwidth from the PSD estimate of each 0% MVC epoch, separately with and without whitening (Welch method, Hamming window, 50% overlap, 614-length DFT). Without whitening we found the 0% MVC bandwidth to be $B_{S,Unwhite} = 118 \pm 72\ Hz$, and with whitening we found the 0% MVC bandwidth to be $B_{S,White} = 329 \pm 157\ Hz$. Fig. 4 plots the fraction of zero values during rest as a function of N_{Eff} and "g".

IV. Discussion

A. Maximum Likelihood Estimates of EMGσ

There has been debate in the literature as to the best way in which to suppress the influence of additive noise when estimating EMGσ. While RDS processing has been suggested (as well as other approaches), no model-derived optimal solution has been peer-review published. Herein, we analytically derived, using maximum likelihood estimation, that constant-effort EMG, modeled as either a Gaussian or Laplacian random process, requires RDS processing when additive noise is modeled [equations (7) and (13), respectively, with $g = 1$]. Further, our work shows that when the particular instance of the EMG signal is such that RDS processing would result in

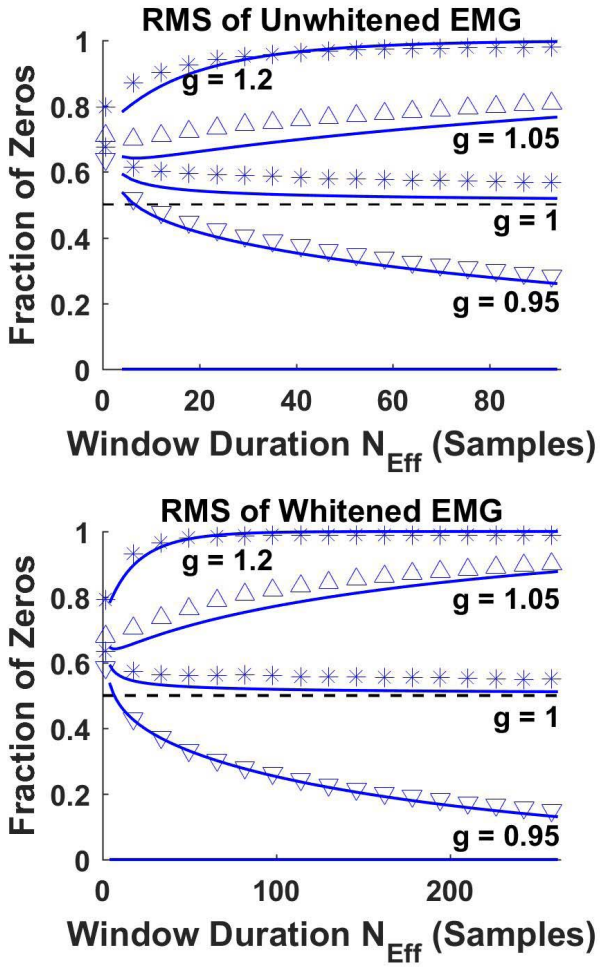

Fig. 4. Symbols show fraction of EMGσ values equal to zero during rest contractions for unwhitened (top) and whitened (bottom) experimental moving average RMS estimates as a function of effective number of samples N_{Eff}, for four different noise gain values "g". Solid lines show corresponding theoretic probabilities of zero values (same as Fig. 1), for comparison. Dash line show 0.5 probability.

a negative value within the square root, then EMGσ should be estimated as EMGσ = 0. While these formulae are derived with constant-effort assumptions, existing EMG processors assume a quasi-stationary EMG signal, even during highly dynamic contractions [30], [53]–[56]. Thus, a moving average window assumes a constant EMGσ within that window, but an EMGσ that slowly varies between adjacent windows. Hence, these RDS processing results remain valid.

B. EMG Probability Density Function

It does not appear that the PDF of rest EMG has previously been reported. We found this PDF to closely match the Gaussian PDF.

But, the literature has variously reported the PDF of active EMG as Gaussian or as more peaked near zero than Gaussian (e.g., Laplacian), mostly in small sample size studies. Roesler [57] (sample size not listed, perhaps one subject; biceps, triceps and forearm muscles) found the EMG PDF to be precisely Gaussian across a range of isometric contraction levels. Parker *et al.* [35] (sample size not listed, likely one trial reported; intramuscular fine wires within the long head of the biceps brachii) found the EMG PDF to be Gaussian during an ∼25% MVC and a just perceptible contraction. Hunter *et al.* [58] (one subject; biceps brachii muscle) found 30% MVC to have a PDF that is more peaked than Gaussian, as did Bilodeau *et al.* [59] for 20% MVCs (16 subjects; biceps brachii and brachioradialis muscles). Nazarpour *et al.* [60] (four subjects; abductor pollicis brevis and flexor carpi radialis muscles) found evidence that the PDF was more peaked (i.e., closer to Laplacian) at low level contractions, but more bell-shaped/Gaussian at higher contraction levels. They postulated that, since more motor unit firings contribute to the EMG during higher contraction levels, the interference signal more closely obeys the central limit theorem—resulting in a more Gaussian shape.

Our own prior work [7] (24 subjects; all distinct from the subjects in the present study) found the PDF from biceps and triceps muscle EMG to be closer to Gaussian than Laplacian, for 10, 25, 50 and 75% constant-force MVCs, using apparatus and methods quite similar to that of the present study. However, this work found that MAV processing produced a higher SNR than RMS processing. A simulation study of constant-effort EMG confirmed that as the EMG PDF is progressively varied from Laplacian to Gaussian, there exists a region wherein the data are more Gaussian in distribution, but MAV processing performs better than RMS.

The present study likely reports the largest sample size to-date. Our EMG exhibited a distribution that closely matched the Gaussian PDF, with a poorer fit to the Laplacian PDF. Since our data were from 50% MVCs (a high contraction level), this result is consistent with the findings of Nazarpour *et al.* [60]. Future comparison to data at lower contraction levels (in which [60] found a more peaked PDF) may be appropriate. The similarity in PDF shapes to our own prior work [7] may be due to the similarity in equipment and use of the identical contraction level. In the end, various factors may influence the EMG PDF, including: electrode shape, size and inter-electrode distance; contraction level; and muscle studied.

C. EMGσ Estimates

Our root mean square error results from the amplitude-modulated ramp contractions show that noise correction is most important at the lowest contractions levels. RDS processing has the advantage of being progressively less noticeable as effort level increases. For example, once the true EMGσ is four times that of the noise standard deviation, the RDS adjustment is only one sixteenth of the true EMGσ. Once the true EMGσ is five times the noise standard deviation, RDS adjustment is only one 25th the true EMGσ. Etc.

D. Estimator Performance During Rest

For the ML estimate (c.f., $g = 1$ in Fig. 1 and Fig. 4), we have shown that approximately 50% of EMGσ estimates will be zero, based on either the Gaussian or Laplacian model (excluding unrealistically small N_{Eff} values). Accordingly, nearly half of all EMGσ estimates will be *greater* than zero during rest! In some applications, this result is problematic. For example, the pose of myoelectrically-controlled

prostheses, orthoses and exoskeletons would slowly drift at rest, producing an undesired and potentially dangerous action. Thus, we suggest that undesired non-zero EMGσ estimates during rest be eliminated by accentuating the noise standard deviation (i.e., setting $g > 1$). Fig. 1 shows that even modest increases in the gain factor g result in much lower probability of a non-zero value. Indeed, it is common to include threshold subtraction in a prosthesis EMG processor (with zero as the boundary condition), although it is currently applied by subtracting the noise standard deviation from EMG RMS (or MAV) and not via RDS processing [61], [62].

Note that many biomechanics studies in which the subject is active most of the time might *not* want to increase the gain factor "g". Doing so might create a bias in EMGσ-force estimates.

E. Limitations

Our theoretical models assumed independent samples, which are approximated in experimental analysis via whitening. However, since signal and noise have some distinctions in their spectral shape (noise exhibits a lower span of power across frequency [3]), one filter cannot precisely whiten both the noise-free EMG signal and the noise. In particular, whitening filters calibrated to active EMG may contain excessive high frequency gain [45]. Thus, some signal correlation will remain. This dissonance may place practical limits on the bandwidth of whitening filters [50], and might argue for the use of RDS processing in concert with other noise mitigation techniques such as adaptive whitening [3] —in which an adaptive Wiener filter provides lowpass filtering with a progressively lower cutoff at lower EMGσ levels.

When evaluating the fraction of zero EMGσ values during a rest contraction, we used that same rest contraction to estimate the noise variance $\left(q^2\right)$. In practice, q^2 may vary over time; thus, so would the fraction of zero EMGσ values during rest. Hence, setting the noise gain factor "g" above one might help to mitigate unmeasured changes in q^2.

V. Conclusion

Using established stochastic models for EMG in the presence of additive noise, we derived that RDS processing represents the ML estimate of EMGσ, under both Gaussian and Laplacian PDF assumptions. We concomitantly showed that EMGσ should be set to zero whenever RDS processing produces a negative-valued result. Further, we showed that the ML estimate at rest produces zero EMGσ estimates only 50% of the time (for all but short-duration smoothing windows). Experimentally, our biceps-triceps EMG data more closely followed a Gaussian PDF than a Laplacian PDF. Our EMGσ estimates closely followed theoretical predictions, both during ramp and rest contractions. This work definitively argues that EMG processors should use RDS processing rather than subtracting the noise standard deviation from EMG RMS (or MAV).

References

[1] E. Kaiser and I. Petersen, "Adaptive filter for EMG control signals," in *The Control Upper-Extremity Prostheses Orthoses*, P. Herberts, R. Kadefors, R. Magnusson, and I. Petersen, Eds., Springfield, IL, USA: Thomas, 1974, pp. 54–57.

[2] N. Hogan and R. W. Mann, "Myoelectric signal processing: Optimal estimation applied to electromyography—Part I: Derivation of the optimal myoprocessor," *IEEE Trans. Biomed. Eng.*, vol. BME-27, no. 7, pp. 382–395, Jul. 1980.

[3] E. A. Clancy and K. A. Farry, "Adaptive whitening of the electromyogram to improve amplitude estimation," *IEEE Trans. Biomed. Eng.*, vol. 47, no. 6, pp. 709–719, Jun. 2000.

[4] N. Hogan and R. W. Mann, "Myoelectric signal processing: Optimal estimation applied to electromyography—Part II: Experimental demonstration of optimal myoprocessor performance," *IEEE Trans. Biomed. Eng.*, vol. BME-27, no. 7, pp. 396–410, Jul. 1980.

[5] E. A. Clancy and N. Hogan, "Single site electromyograph amplitude estimation," *IEEE Trans. Biomed. Eng.*, vol. 41, no. 2, pp. 159–167, Feb. 1994.

[6] E. A. Clancy and N. Hogan, "Multiple site electromyograph amplitude estimation," *IEEE Trans. Biomed. Eng.*, vol. 42, no. 2, pp. 203–211, Feb. 1995.

[7] E. A. Clancy and N. Hogan, "Probability density of the surface electromyogram and its relation to amplitude detectors," *IEEE Trans. Biomed. Eng.*, vol. 46, no. 6, pp. 730–739, Jun. 1999.

[8] C. Dai, B. Bardizbanian, and E. A. Clancy, "Comparison of constant-posture force-varying EMG-force dynamic models about the elbow," *IEEE Trans. Neural Syst. Rehabil. Eng.*, vol. 25, no. 9, pp. 1529–1538, Sep. 2017.

[9] C. Dai, Z. Zhu, C. Martinez-Luna, T. R. Hunt, T. R. Farrell, and E. A. Clancy, "Two degrees of freedom, dynamic, hand-wrist EMG-force using a minimum number of electrodes," *J. Electromyogr. Kinesiol.*, vol. 47, pp. 10–18, Aug. 2019.

[10] D. Staudenmann, K. Roeleveld, D. F. Stegeman, and J. H. van Dieën, "Methodological aspects of SEMG recordings for force estimation—A tutorial and review," *J. Electromyogr. Kinesiol.*, vol. 20, no. 3, pp. 375–387, 2010.

[11] J. Hashemi, E. Morin, P. Mousavi, K. Mountjoy, and K. Hashtrudi-Zaad, "EMG–force modeling using parallel cascade identification," *J. Electromyogr. Kinesiol.*, vol. 22, no. 3, pp. 469–477, Jun. 2012.

[12] J. Hashemi, E. Morin, P. Mousavi, and K. Hashtrudi-Zaad, "Enhanced dynamic EMG-force estimation through calibration and PCI modeling," *IEEE Trans. Neural Syst. Rehabil. Eng.*, vol. 23, no. 1, pp. 41–50, Jan. 2015.

[13] E. P. Doheny, M. M. Lowery, D. P. FitzPatrick, and M. J. O'Malley, "Effect of elbow joint angle on force–EMG relationships in human elbow flexor and extensor muscles," *J. Electromyogr. Kinesiol.*, vol. 18, no. 5, pp. 760–770, Oct. 2008.

[14] C. Dai, S. Martel, F. Martel, D. Rancourt, and E. A. Clancy, "Single-trial estimation of quasi-static EMG-to-joint-mechanical-impedance relationship over a range of joint torques," *J. Electromyogr. Kinesiol.*, vol. 45, pp. 18–25, Apr. 2019.

[15] C. J. Abul-Haj and N. Hogen, "Functional assessment of control systems for cybernetic elbow prostheses. I. Description of the technique," *IEEE Trans. Biomed. Eng.*, vol. 37, no. 11, pp. 1025–1036, Nov. 1990.

[16] D. Shin, J. Kim, and Y. Koike, "A myokinetic arm model for estimating joint torque and stiffness from EMG signals during maintained posture," *J. Neurophysiol.*, vol. 101, no. 1, pp. 387–401, 2009.

[17] T. Kawase, H. Kambara, and Y. Koike, "A power assist device based on joint equilibrium point estimation from EMG signals," *J. Robot. Mechatron.*, vol. 24, no. 1, pp. 205–218, 2012.

[18] S. Pfeifer, H. Vallery, M. Hardegger, R. Riener, and E. J. Perreault, "Model-based estimation of knee stiffness," *IEEE Trans. Biomed. Eng.*, vol. 59, no. 9, pp. 2604–2612, Sep. 2012.

[19] M. A. Golkar, E. S. Tehrani, and R. E. Kearney, "Linear parameter varying identification of dynamic joint stiffness during time-varying voluntary contractions," *Front. Comput. Neurosci.*, vol. 11, p. 35, May 2017.

[20] D. J. Ostry and A. G. Feldman, "A critical evaluation of the force control hypothesis in motor control," *Exp. Brain Res.*, vol. 153, no. 3, pp. 275–288, 2003.

[21] P. Parker, K. Englehart, and B. Hudgins, "Myoelectric signal processing for control of powered limb prostheses," *J. Electromyogr. Kinesiol.*, vol. 16, no. 6, pp. 541–548, Dec. 2006.

[22] D. Farina *et al.*, "The extraction of neural information from the surface EMG for the control of upper-limb prostheses: Emerging avenues and challenges," *IEEE Trans. Neural Syst. Rehabil. Eng.*, vol. 22, no. 4, pp. 797–809, Jul. 2014.

[23] R. A. Popat *et al.*, "Quantitative assessment of four men using above-elbow prosthetic control," *Arch. Phys. Med. Rehabil.*, vol. 74, no. 7, pp. 720–729, Jul. 1993.

[24] G. M. Hagg, B. Melin, and R. Kadefors, "Applications in ergonomics," in *Electromyography: Physiology, Engineering, and Non-Invasive Applications*, R. Merletti and P. A. Parker, Eds. Hoboken, NJ, USA: Wiley, 2004, pp. 343–363.

[25] S. Kumar and A. Mital, *Electromyography in Ergonomics*. Briston, U.K.: Taylor & Francis, 1996.

[26] C. Disselhorst-Klug, T. Schmitz-Rode, and G. Rau, "Surface electromyography and muscle force: Limits in sEMG-force relationship and new approaches for applications," *Clin. Biomech.*, vol. 24, no. 3, pp. 225–235, Aug. 2009.

[27] C. A. M. Doorenbosch and J. Harlaar, "A clinically applicable EMG–force model to quantify active stabilization of the knee after a lesion of the anterior cruciate ligament," *Clin. Biomech.*, vol. 18, no. 2, pp. 142–149, 2003.

[28] R. Merletti, A. Botter, and U. Barone, "Detection and conditioning of surface EMG signals," in *Surface Electromyography: Physiology, Engineering, and Applications*, R. Merletti and D. Farina, Eds. Hoboken, NJ, USA: Wiley, 2016, pp. 54–90.

[29] E. A. Clancy, E. L. Morin, and R. Merletti, "Sampling, noise-reduction and amplitude estimation issues in surface electromyography," *J. Electromyograph. Kinesiol.*, vol. 12, no. 1, pp. 1–16, Feb. 2002.

[30] E. A. Clancy, "Electromyogram amplitude estimation with adaptive smoothing window length," *IEEE Trans. Biomed. Eng.*, vol. 46, no. 6, pp. 717–729, Jun. 1999.

[31] E. A. Clancy, D. Farina, and R. Merletti, "Cross-comparison of time- and frequency-domain methods for monitoring the myoelectric signal during a cyclic, force-varying, fatiguing hand-grip task," *J. Electromyogr. Kinesiol.*, vol. 15, no. 3, pp. 256–265, 2005.

[32] P. Liu, L. Liu, F. Martel, D. Rancourt, and E. A. Clancy, "Influence of joint angle on EMG–torque model during constant-posture, quasi-constant-torque contractions," *J. Electromyogr. Kinesiol.*, vol. 23, no. 5, pp. 1020–1028, Oct. 2013.

[33] P. Liu, L. Liu, and E. A. Clancy, "Influence of joint angle on EMG-torque model during constant-posture, torque-varying contractions," *IEEE Trans. Neural Syst. Rehabil. Eng.*, vol. 23, no. 6, pp. 1039–1046, Nov. 2015.

[34] E. A. Clancy, C. Martinez-Luna, M. Wartenberg, C. Dai, and T. R. Farrell, "Two degrees of freedom quasi-static EMG-force at the wrist using a minimum number of electrodes," *J. Electromyogr. Kinesiol.*, vol. 34, pp. 24–36, Jun. 2017.

[35] P. A. Parker, J. A. Stuller, and R. N. Scott, "Signal processing for the multistate myoelectric channel," *Proc. IEEE*, vol. 65, no. 5, pp. 662–674, May 1977.

[36] Y. T. Zhang, P. A. Parker, and R. N. Scott, "Control performance characteristics of myoelectric signal with additive interference," *Med. Biol. Eng. Comput.*, vol. 29, no. 1, pp. 84–88, Jan. 1991.

[37] P. A. Parker and R. N. Scott, "Myoelectric control of prostheses," *Crit. Rev. Biomed. Eng.*, vol. 13, no. 4, pp. 283–310, 1985.

[38] P. Bonato, T. D'Alessio, and M. Knaflitz, "A statistical method for the measurement of muscle activation intervals from surface myoelectric signal during gait," *IEEE Trans. Biomed. Eng.*, vol. 45, no. 3, pp. 287–299, Mar. 1998.

[39] R. Baratta, M. Solomonow, B.-H. Zhou, and M. Zhu, "Methods to reduce the variability of EMG power spectrum estimates," *J. Electromyogr. Kinesiol.*, vol. 8, no. 5, pp. 279–285, Oct. 1998.

[40] K. Koirala, M. Dasog, P. Liu, and E. A. Clancy, "Using the electromyogram to anticipate torques about the elbow," *IEEE Trans. Neural Syst. Rehabil. Eng.*, vol. 23, no. 3, pp. 396–402, May 2015.

[41] L. Frey Law, C. Krishnan, and K. Avin, "Modeling nonlinear errors in surface electromyography due to baseline noise: A new methodology," *J. Biomech.*, vol. 44, no. 1, pp. 202–205, Jan. 2011.

[42] R. Ortengren, "Noise and artefacts," in *Electromyography in Ergonomics*, S. Kumar and A. Mital, Eds., London, U.K.: Taylor & Francis, 1996, pp. 97–107.

[43] G.-A. Hansson, "Letter to the editor," *J. Biomech.*, vol. 44, p. 1637, 2011.

[44] L. Frey Law, K. Avin, and C. Krishnan, "Response to letter to the editor," *J. Biomech.*, vol. 44, pp. 1637–1638, 2011.

[45] E. A. Clancy, "Stochastic modeling of the relationship between the surface electromygram and muscle torque," Ph.D. dissertation, Dept. Elect. Eng. Comput. Sci., Massachusetts Inst. Technol., Cambridge, MA, USA, 1991, pp. 303–352 and 449–469.

[46] H. Wang, "Optimal electromyogram modeling and processing during active contractions and rest," M.S. thesis, Worcester Polytech. Inst., Worcester, MA, USA, 2019, pp. 40–58.

[47] G. B. Thomas, Jr., M. D. Weir, J. Hass, and C. Heil, *Thomas' Calculus*, 13th ed. Boston, MA, USA: Pearson, 2014, pp. 185–193.

[48] A. W. Drake, *Fundamentals of Applied Probability Theory*. New York, NY, USA: McGraw-Hill, 1967, pp. 103–107 and 273–274.

[49] P. Prakash, C. A. Salini, J. A. Tranquilli, D. R. Brown, and E. A. Clancy, "Adaptive whitening in electromyogram amplitude estimation for epoch-based applications," *IEEE Trans. Biomed. Eng.*, vol. 52, no. 2, pp. 331–334, Feb. 2005.

[50] M. Dasog, K. Koirala, P. Liu, and E. A. Clancy, "Electromyogram bandwidth requirements when the signal is whitened," *IEEE Trans. Neural Sys. Rehabil. Eng.*, vol. 22, no. 3, pp. 664–670, May 2014.

[51] J. S. Bendat and A. G. Piersol, *Random Data: Analysis and Measurement Procedures*. New York, NY, USA: Wiley, 1971, pp. 277–281.

[52] L. Liu, P. Liu, E. A. Clancy, E. Scheme, and K. B. Englehart, "Electromyogram whitening for improved classification accuracy in upper limb prosthesis control," *IEEE Trans. Neural Syst. Rehabil. Eng.*, vol. 21, no. 5, pp. 767–774, Sep. 2013.

[53] R. B. Jerard, T. W. Williams, and C. W. Ohlenbusch, "Practical design of an EMG controlled above elbow prosthesis," in *Proc. Conf. Eng. Devices Rehabil.*, Boston, MA, USA, 1974, pp. 73–77.

[54] T. D'Alessio, "Analysis of a digital EMG signal processor in dynamic conditions," *IEEE Trans. Biomed. Eng.*, vol. BME-32, no. 1, pp. 78–82, Jan. 1985.

[55] E. Park and S. G. Meek, "Adaptive filtering of the electromyographic signal for prosthetic control and force estimation," *IEEE Trans. Biomed. Eng.*, vol. 42, no. 10, pp. 1048–1052, Oct. 1995.

[56] S. Ranaldi, C. De Marchis, and S. Conforto, "An automatic, adaptive, information-based algorithm for the extraction of the sEMG envelope," *J. Electromyogr. Kinesiol.*, vol. 42, pp. 1–9, Oct. 2018.

[57] H. Roesler, "Statistical analysis and evaluation of myoelectric signals for proportional control," in *The Control Upper-Extremity Prosthesis Orthoses*. Springfield, IL, USA: Thomas, 1974, pp. 44–53.

[58] I. W. Hunter, R. E. Kearney, and L. A. Jones, "Estimation of the conduction velocity of muscle action potentials using phase and impulse response function techniques," *Med. Biol. Eng. Comput.*, vol. 25, no. 2, pp. 121–126, Mar. 1987.

[59] M. Bilodeau, M. Cincera, A. B. Arsenault, and D. Gravel, "Normality and stationarity of EMG signals of elbow flexor muscles during ramp and step isometric contractions," *J. Electromyogr. Kinesiol.*, vol. 7, no. 2, pp. 87–96, Jun. 1997.

[60] K. Nazarpour, A. H. Al-Timemy, G. Bugmann, and A. Jackson, "A note on the probability distribution function of the surface electromyogram signal," *Brain Res. Bull.*, vol. 90, pp. 88–91, Jan. 2013.

[61] T. W. Williams, III, "Practical methods for controlling powered upper-extremity prostheses," *Assist. Technol.*, vol. 2, no. 1, pp. 3–18, 1990.

[62] J. M. Hahne, M. A. Schweisfurth, M. Koppe, and D. Farina, "Simultaneous control of multiple functions of bionic hand prostheses: Performance and robustness in end users," *Sci. Robot.*, vol. 3, Jun. 2018, Art. no. eaat3630.